AD-A204 975

DOCUMENTATION PAGE

Form Approved
OMB No. 0704-0188

1a. REPORT SECURITY CLASSIFICATION Unclassified	1b. RESTRICTIVE MARKINGS None
2a. SECURITY CLASSIFICATION AUTHORITY	3. DISTRIBUTION/AVAILABILITY OF REPORT Approved for public release; Distribution is unlimited.
2b. DECLASSIFICATION/DOWNGRADING SCHEDULE	
4. PERFORMING ORGANIZATION REPORT NUMBER(S) JA 220:038:88	5. MONITORING ORGANIZATION REPORT NUMBER(S) JA 220:038:88
6a. NAME OF PERFORMING ORGANIZATION Naval Ocean Research and Development Activity 6b. OFFICE SYMBOL (If applicable) 244	7a. NAME OF MONITORING ORGANIZATION Ocean Acoustics and Technology Directorate
6c. ADDRESS (City, State, and ZIP Code) Stennis Space Center, MS 39529-5004	7b. ADDRESS (City, State, and ZIP Code) Stennis Space Center, MS 39529-5004
8a. NAME OF FUNDING/SPONSORING ORGANIZATION NORDA/ONR 8b. OFFICE SYMBOL (If applicable) 244	9. PROCUREMENT INSTRUMENT IDENTIFICATION NUMBER
8c. ADDRESS (City, State, and ZIP Code) Stennis Space Center, MS 39529-5004	10. SOURCE OF FUNDING NUMBERS PROGRAM ELEMENT NO. 61153N; PROJECT NO. 3205; TASK NO. 330; WORK UNIT ACCESSION NO.

11. TITLE (Include Security Classification)

Low-Frequency, Bottom-Interacting Pulse Propagation in Range-Dependent Oceans

12. PERSONAL AUTHOR(S)
Michael D. Collins

13a. TYPE OF REPORT	13b. TIME COVERED	14. DATE OF REPORT (Year, Month, Day)	15. PAGE COUNT
Journal Article	FROM _____ TO _____	October 1988	7

16. SUPPLEMENTARY NOTATION

17. COSATI CODES			18. SUBJECT TERMS (Continue on reverse if necessary and identify by block number)
FIELD	GROUP	SUB-GROUP	Reprints; Parabolic Pulse; Attenuation; Density

19. ABSTRACT (Continue on reverse if necessary and identify by block number)

An asymptotic-numerical model for low-frequency, bottom-interacting pulse propagation in the ocean is derived. The model works in the time domain using an approach analogous to the parabolic equation method that is commonly used in the frequency domain. The model handles depth and range variations in the speed of sound, density, and attenuation. The attenuation is assumed to depend linearly on frequency in the sediment. The accuracy of the model is demostrated with a benchmark. Keywords:

20 DISTRIBUTION/AVAILABILITY OF ABSTRACT	21. ABSTRACT SECURITY CLASSIFICATION
☐ UNCLASSIFIED/UNLIMITED ☒ SAME AS RPT. ☐ DTIC USERS	Unclassified
22a. NAME OF RESPONSIBLE INDIVIDUAL Bob Field	22b. TELEPHONE (Include Area Code) (601) 688-4648 22c. OFFICE SYMBOL 244

DD Form 1473, JUN 86 — Previous editions are obsolete. — SECURITY CLASSIFICATION OF THIS PAGE

Unclassified

J-OE 13 4 24069

Low-Frequency, Bottom-Interacting Pulse Propagation in Range-Dependent Oceans

Michael D. Collins

Reprinted from
IEEE JOURNAL OF OCEANIC ENGINEERING
Vol. 13, No. 4, October 1988

Low-Frequency, Bottom-Interacting Pulse Propagation in Range-Dependent Oceans

MICHAEL D. COLLINS

(Invited Paper)

Abstract—**An asymptotic-numerical model for low-frequency, bottom-interacting pulse propagation in the ocean is derived. The model works in the time domain using an approach analogous to the parabolic equation method that is commonly used in the frequency domain. The model handles depth and range variations in the speed of sound, density, and attenuation. The attenuation is assumed to depend linearly on frequency in the sediment. The accuracy of the model is demonstrated with a benchmark.**

Keywords—**parabolic, pulse, attenuation, density.**

I. Introduction

RANGE-DEPENDENT propagation problems can be solved efficiently with the parabolic equation (PE) method. It is most useful for low-frequency problems because the number of operations required for the numerical solution of the PE increases with the frequency squared for two-dimensional problems. The PE method was first applied to underwater acoustics by Tappert [1], who also provided a historical account of the PE method. For this application, the PE method has been highly developed. In its present state, it can handle density variations [2]–[4], range dependence [5], three-dimensional variations [6]–[8], and wide-angle propagation [9], [10]. The accuracy of the PE method has been demonstrated with many benchmark comparisons using normal mode and other results [11].

Pulse propagation problems can be solved with frequency-domain methods by solving for one frequency at a time and summing the results. The PE method [12], [13], the fast-field program [14], and the WKB method [15], [16] have been used in this fashion. These approaches can probably be improved substantially for broadband pulses by working in the time domain because a significant amount of effort must be devoted to managing the component frequencies and performing the sums with the frequency-domain approach. Since range-dependent problems are frequently of interest, a time-domain approach analogous to the PE method would be very useful. Two such models exist, the nonlinear progressive wave equation (NPE) [17], which is an initial value problem in time, and the time-domain parabolic equation TDPE [18]–[20], which is an initial value problem in range. In contrast to the PE method, these models have not been fully developed.

Manuscript received January 29, 1988; revised July 15, 1988. This work was supported by ONR and NORDA.

The author is with the Naval Ocean Research and Development Activity, Stennis Space Center, MS 39529.

IEEE Log Number 8824069.

The need for the development of bottom interaction capability into these modes was the motivation for the present study. A robust numerical solution was developed for the NPE [17], and it seems more natural to march a solution of the wave equation in time rather than range. Thus, we work with the NPE rather than the TDPE. Since the nonlinear term in the NPE is dropped, we do not adhere to the terminology for this model and refer to the linear version of the NPE as the progressive wave equation (PWE). The number of operations required for the numerical solution of the PWE increases with the frequency cubed. Thus, this model is best suited to handle low-frequency problems.

II. Derivation of the PWE

We neglect attenuation for now and begin with the following wave equation due to Bergmann [21] for the acoustic pressure P:

$$\rho \nabla \cdot \left(\frac{1}{\rho} \nabla P \right) = \frac{1}{c^2} \frac{\partial^2 P}{\partial t^2} \tag{1}$$

where t is time, c is sound speed, and ρ is density. Azimuthal dependence is ignored, and cylindrical coordinates are used with z being the depth below the ocean surface and r being the horizontal distance from a point sound source at $z = z_0$. The dimensions of the independent variables have been removed using the factors $c_0 = c(z_0), \rho_0 = \rho(z_0)$, and the characteristic time scale τ of the source function $F(t)$. Cylindrical spreading applies for large r because the ocean acts as a waveguide. Thus, spreading can be handled by defining $p = r^{1/2} P$. We let $r_0 \gg 1$, assume $| \partial \rho / \partial r | \ll | \partial \rho / \partial z |$, and approximate (1) for $r > r_0$ by

$$\frac{\partial^2 p}{\partial z^2} - \frac{1}{\rho} \frac{\partial \rho}{\partial z} \frac{\partial p}{\partial z} + \frac{\partial^2 p}{\partial r^2} = \frac{1}{c^2} \frac{\partial^2 p}{\partial t^2}. \tag{2}$$

Following the approach used to derive the TDPE and the NPE, we introduce a reference frame moving outward at the reference speed c_0 with the new independent variable $s = r - c_0 t$ and new dependent variable

$$u(s, z, t) = p(s + c_0 t, z, t). \tag{3}$$

With these definitions, (2) becomes

$$\frac{\partial^2 u}{\partial z^2} - \frac{1}{\rho} \frac{\partial \rho}{\partial z} \frac{\partial u}{\partial z} + \left(1 - \frac{c_0^2}{c^2} \right) \frac{\partial^2 u}{\partial s^2} + \frac{2 c_0}{c^2} \frac{\partial^2 u}{\partial s \partial t} = \frac{1}{c^2} \frac{\partial^2 u}{\partial t^2}. \tag{4}$$

0364-9059/88/1000-0222$01.00

The PE method is based on the small-angle asymptotic limit. Long-range propagation in the ocean results in nearly vertical wavefronts due to the fact that wide-angle rays are not trapped by the oceanic waveguide. In other words, energy propagation is limited to within the angle Φ of the horizontal, where $\epsilon = \tan^2 \Phi \ll 1$. For the plane wave

$$u(s, z, t) = f[s \cos\phi + z \sin\phi + (\cos\phi - 1)c_0 t] \quad (5)$$

with $|\phi| < \Phi$, we observe that $\partial u/\partial t = O(\epsilon)$ and $\partial u/\partial z = O(\epsilon^{1/2})$.

We assume that $c = c_0 + O(\epsilon)$, $\rho(r, z) = \rho'(r\psi, z\epsilon^{1/2})$, $r > r_0 = O(\epsilon^{-1})$, and $c_0\tau/d = O(\epsilon^{1/2})$, where ρ' is independent of ϵ, $\psi \ll \epsilon$, and d is the ocean depth. Using the scales suggested by the above discussion, we assume that $u(s, z, t) = u'(s, z\epsilon^{1/2}, t\epsilon)$, where u' is independent of ϵ. This results in $\partial u/\partial t = O(\epsilon)$ and $\partial u/\partial z = O(\epsilon^{1/2})$. An analogous scaling is commonly used in the frequency domain for deriving the PE [1], [4]. To leading order in ϵ, the approximation made in going from (1) to (2) is valid and (4) becomes

$$\frac{c_0}{2}\left(\frac{\partial^2 u}{\partial z^2} - \frac{1}{\rho}\frac{\partial \rho}{\partial z}\frac{\partial u}{\partial z}\right) + (c - c_0)\frac{\partial^2 u}{\partial s^2} + \frac{\partial^2 u}{\partial s \partial t} = 0. \quad (6)$$

We assume u has compact support in s for all time and integrate (6) with respect to s to obtain the PWE

$$\frac{\partial u}{\partial t} = \frac{c_0}{2}\int_s^\infty \left(\frac{\partial^2 u}{\partial z^2} - \frac{1}{\rho}\frac{\partial \rho}{\partial z}\frac{\partial u}{\partial z}\right) ds' + (c_0 - c)\frac{\partial u}{\partial s}. \quad (7)$$

III. The Loss Term

Let $\eta = (40\pi \log_{10} e)^{-1}$ and β be the attenuation in decibels per wavelength with $\eta\beta = O(\epsilon)$. For the circular frequency ω, the complex wavenumber $K = k(1 + i\eta\beta)$ is assumed in the sediment, where the $O(1)$ wavenumber $k = \omega/c$. This formulation is used to model attenuation that increases linearly with frequency, which is in agreement with experimental results [22]–[24] involving various materials and frequencies. The linear dependence has been challenged [25], [26]. However, the model we derive can be modified to handle a general frequency dependence.

The dependent variable p in (2) is replaced with U, which is defined by

$$p(r, z, t) = U(r, z)\exp(ik_0 s) \quad (8)$$

with the assumption $U(r, z) = U'(r\epsilon, z\epsilon^{1/2})$, where $k_0 = \omega/c_0$ and U' is independent of ϵ. Substituting (8) into (2) and retaining leading-order terms, we obtain the following PE, which is valid for $r > r_0$:

$$\frac{\partial U}{\partial r} = \frac{i}{2k_0}\left(\frac{\partial^2 U}{\partial z^2} - \frac{1}{\rho}\frac{\partial \rho}{\partial z}\frac{\partial U}{\partial z}\right) + i(k - k_0)U - \eta\beta k_0 U. \quad (9)$$

In the absence of the other operators on the right-hand side of (9), the loss operator $-\eta\beta k_0 U$ acts over the range increment Δr as follows:

$$U(r, z)\exp(ik_0 s) \to U(r, z)\exp(ik_0 s - \eta\beta k_0 \Delta r) \quad \text{as } r \to r + \Delta r. \quad (10)$$

The coefficient function U, which depends weakly on r and z, is ignored. The loss operator is valid to leading order because it is correct in the limit $\Phi \to 0$.

In the time domain, the Fourier transform is applied to decompose the signal as follows:

$$u(s, z, t) = \int_{-\infty}^{\infty} \hat{u}(k, z, t)\exp(iks)dk \quad (11)$$

$$\hat{u}(k, z, t) = \frac{1}{2\pi}\int_{-\infty}^{\infty} u(s, z, t)\exp(-iks)ds. \quad (12)$$

It follows from (12) that $\partial\hat{u}/\partial t = O(\epsilon)$ and $\partial\hat{u}/\partial z = O(\epsilon^{1/2})$. In (11), the field is written as a superposition of plane waves each multiplied by a function depending weakly on t and z. A discrete loss operator analogous to (10) would act over the time increment Δt as follows:

$$u(s, z, t) \to \int_{-\infty}^{\infty} \hat{u}(k, z, t)\exp(iks - \eta\beta \mid k \mid c_0\Delta t)dk \quad \text{as } t \to t + \Delta t. \quad (13)$$

Once again, the coefficient function of the plane wave is ignored, and the loss operator is valid to leading order because it is correct in the limit $\Phi \to 0$. Substituting (12) into (13) and interchanging the order of integration, we obtain

$$u(s, z, t) \to \frac{\eta\beta c_0 \Delta t}{\pi}\int_{-\infty}^{\infty} \frac{u(s', z, t)\, ds'}{(\eta\beta c_0\Delta t)^2 + (s' - s)^2} \quad \text{as } t \to t + \Delta t. \quad (14)$$

A continuous loss operator L is obtained by taking the limit in (14) to obtain

$$Lu = \lim_{\Delta t \to 0}\left[\frac{\eta\beta c_0}{\pi}\int_{-\infty}^{\infty} \frac{u(s', z, t)\, ds'}{(\eta\beta c_0\Delta t)^2 + (s' - s)^2} - \frac{u(s, z, t)}{\Delta t}\right] \quad (15)$$

$$Lu = \lim_{\Delta t \to 0}\frac{\eta\beta c_0}{\pi}\int_{-\infty}^{\infty} \frac{u(s', z, t) - u(s, z, t)}{(\eta\beta c_0\Delta t)^2 + (s' - s)^2} ds'. \quad (16)$$

In going from (15) to (16), we have used the identity

$$\frac{\eta\beta c_0 \Delta t}{\pi}\int_{-\infty}^{\infty} \frac{ds'}{(\eta\beta c_0\Delta t)^2 + (s' - s)^2} = 1. \quad (17)$$

The limit in (16) exists as the Cauchy principal value of the integral with $\Delta t = 0$.

Adding Lu to (7), we obtain the PWE

$$\frac{\partial u}{\partial t} = \frac{c_0}{2}\int_s^\infty \left(\frac{\partial^2 u}{\partial z^2} - \frac{1}{\rho}\frac{\partial \rho}{\partial z}\frac{\partial u}{\partial z}\right) ds' + (c_0 - c)\frac{\partial u}{\partial s} + \frac{\eta\beta c_0}{\pi}\int_{-\infty}^{\infty} \frac{u(s', z, t) - u(s, z, t)}{(s' - s)^2} ds'. \quad (18)$$

This PWE differs from the NPE of [17] by the presence of the density and attenuation terms and the absence of the nonlinear and spreading terms. The integral operator appearing in (18)

is of the Kramers–Krönig type [27]. The approach we have described can be generalized to handle an arbitrary complex dispersion relation by replacing the function $\eta\beta \mid k \mid$ in (13) by a complex function of k.

IV. Numerical Solution of the PWE

The domain is discretized with grid spacings $\Delta s, \Delta z$, and Δt. The ocean surface at $z = 0$ is assumed to be pressure release, and the signal is assumed to be trapped within $\Gamma = (0, s_{\max}) \times (0, z_{\max})$ due to the moving frame and the lossy bottom. Thus, the boundary condition $u = 0$ is imposed on $\partial\Gamma$. The ocean depth is assumed constant over Γ. This is a valid leading-order approximation if range dependence is sufficiently gradual.

We solve (18) numerically using the method of alternating directions, which was used to solve the NPE [17] and requires numerical methods for each of the following:

$$\frac{\partial u}{\partial t} + (c - c_0)\frac{\partial u}{\partial s} = 0 \tag{19}$$

$$\frac{\partial u}{\partial t} = \frac{c_0}{2}\int_s^\infty \left(\frac{\partial^2 u}{\partial z^2} - \frac{1}{\rho}\frac{\partial \rho}{\partial z}\frac{\partial u}{\partial z}\right) ds' \tag{20}$$

$$\frac{\partial u}{\partial t} = \frac{\eta\beta c_0}{\pi}\int_{-\infty}^\infty \frac{u(s', z, t) - u(s, z, t)}{(s' - s)^2}\, ds'. \tag{21}$$

The Lax–Wendroff scheme [28] may be applied to solve the first-order hyperbolic equation (19). The Courant–Friedrichs–Lewy (CFL) condition,

$$\max \mid c - c_0 \mid \Delta t \le \Delta s \tag{22}$$

must be satisfied for stability.

With the imposed boundary conditions, (20) is equivalent to

$$\frac{\partial^2 u}{\partial z^2} - \frac{1}{\rho}\frac{\partial \rho}{\partial z}\frac{\partial u}{\partial z} + \frac{2}{c_0}\frac{\partial^2 u}{\partial s \partial t} = 0. \tag{23}$$

Galerkin's method with linear test functions is applied to discretize depth dependence. The depth grid points are defined by $z_i = i\Delta z$. The basis functions $\Psi_i(z)$ vanish for $\mid z - z_i \mid > \Delta z$, increase linearly from 0 to 1 over $z_{i-1} < z < z_i$, and decrease from 1 to 0 over $z_i < z < z_{i+1}$.

The basis functions can be used to approximate a function by a piecewise linear function with exact agreement at the grid points. We define $u_i(s, t) = u(s, z_i, t)$ and $\rho_i = \rho(z_i)$ and obtain

$$u(s, z, t) \cong \sum_i u_i(s, t)\Psi_i(z) \tag{24}$$

$$\rho(z) \cong \sum_i \rho_i \Psi_i(z). \tag{25}$$

Galerkin's method discretizes depth dependence in (23) by using (24) and (25) and requiring that the following hold for all i:

$$\int \Psi_i(z)\left[\frac{\partial^2 u}{\partial z^2} - \frac{1}{\rho}\frac{\partial \rho}{\partial z}\frac{\partial u}{\partial z} + \frac{2}{c_0}\frac{\partial^2 u}{\partial s \partial t}\right] dz = 0. \tag{26}$$

Substituting (24) and (25) into (26) we obtain

$$A\vec{u} + B\frac{\partial^2 \vec{u}}{\partial s \partial t} = 0 \tag{27}$$

where the vector $\vec{u}(s, t)$ contains the values of u at the depth grid points and A and B are tridiagonal matrices with entries

$$A_{i,i-1} = 2 - \rho_{i-1}\sigma_{i-1/2} \tag{28}$$

$$A_{i,i} = \rho_{i-1}\sigma_{i-1/2} + \rho_{i+1}\sigma_{i+1/2} - 4 \tag{29}$$

$$A_{i,i+1} = 2 - \rho_{i+1}\sigma_{i+1/2} \tag{30}$$

$$\sigma_{i+1/2} = \begin{cases} \dfrac{1}{\rho_i} & \text{if } \rho_i = \rho_{i+1} \\ \dfrac{\log(\rho_{i+1}) - \log(\rho_i)}{\rho_{i+1} - \rho_i} & \text{if } \rho_i \ne \rho_{i+1} \end{cases} \tag{31}$$

$$B_{i,i-1} = \frac{(\Delta z)^2}{3c_0} \tag{32}$$

$$B_{i,i} = \frac{(2\Delta z)^2}{3c_0} \tag{33}$$

$$B_{i,i+1} = \frac{(\Delta z)^2}{3c_0}. \tag{34}$$

We define the grid points $s_j = j\Delta s$ and $t_n = n\Delta t$ and $\vec{u}_{j,n} = \vec{u}(s_j, t_n)$. Integrating (27) over $(s_j, s_{j+1}) \times (t_n, t_{n+1})$ using the trapezoid rule where necessary, we obtain

$$\frac{\Delta s \Delta t}{4} A(\vec{u}_{j+1,n+1} + \vec{u}_{j+1,n} + \vec{u}_{j,n+1} + \vec{u}_{j,n}) + B(\vec{u}_{j+1,n+1} - \vec{u}_{j+1,n} - \vec{u}_{j,n+1} + \vec{u}_{j,n}) = 0. \tag{35}$$

In the case $c \equiv c_0$, $\rho \equiv \rho_0$, and $\beta \equiv 0$, (18) reduces to (20). In this situation, energy flows from $s = s_{\max}$ to $s = 0$ due to geometric dispersion. This physical consideration implies that (35) must be applied by sweeping from $s = s_{\max}$ to $s = 0$, which results in the scheme

$$M\vec{u}_{j,n+1} = \vec{b}_{j,n+1} \tag{36}$$

$$M = B - \frac{\Delta s \Delta t}{4} A \tag{37}$$

$$\vec{b}_{j,n+1} = \frac{\Delta s \Delta t}{4} A(\vec{u}_{j+1,n+1} + \vec{u}_{j+1,n} + \vec{u}_{j,n}) + B(\vec{u}_{j+1,n+1} - \vec{u}_{j+1,n} + \vec{u}_{j,n}). \tag{38}$$

The loss operator is defined by (14) as $\Delta t \to 0$. Thus, (14) is used to solve (21). The CFL condition (22) and accuracy considerations result in $\delta = \eta\beta c_0 \Delta t / \Delta s \ll 1$. (In the example below, $\delta \cong 0.023$.) Thus, the kernel in (14), which approximates a delta function, is nearly singular at $s' = s$. The integral over $(s_i - \Delta s/2, s_i + \Delta s/2)$ is approximated by replacing $u(s, z, t)$ with $u(s_i, z, t)$ and integrating the kernel

analytically to obtain

$$u(s_j, z, t) \to \frac{1}{\pi} \sum_i u(s_i, z, t) \left[\tan^{-1}\left(\frac{i - j + \frac{1}{2}}{\delta} \right) - \tan^{-1}\left(\frac{i - j - \frac{1}{2}}{\delta} \right) \right]. \quad (39)$$

For $i \neq j$, the terms in the sum are of order $\delta/(i-j)^2$. Thus, the sum may be truncated making the loss operator numerically efficient.

V. The Initial Field

The PWE is not valid near the sound source because it is derived from a singular perturbation problem. Both $\partial u/\partial t$ and $1/r$ fail to be $O(\epsilon)$ in a boundary layer near $r = 0$. In the boundary layer and within the angle Φ of the horizontal, rays are not significantly affected by the weak refraction of the ocean. Thus, the PWE may be initialized near the source at $t = t_0$ with

$$p(r, z, t) = \frac{1}{d_-} F\left(t - \frac{d_-}{c_0} \right) - \frac{1}{d_+} F\left(t - \frac{d_+}{c_0} \right) \quad (40)$$

where $d_\pm^2 = r^2 + (z \pm z_0)^2$.

This solution is valid for small r and ϵ because refraction in the ocean is negligible over short ranges, and the propagating rays, which travel within the angle Φ from horizontal, do not intersect the ocean bottom near the source. It breaks down for large r because refraction in the ocean is significant over large ranges, and propagating rays from the source eventually reflect from the ocean bottom.

The numerical method used to solve the PWE requires a continuously differentiable source function with compact support. A source function that approximates a delta function would be useful because it can be used to approximate the impulse response of the ocean. The Gaussian source function $G_\nu(t) = \exp[-(\nu t)^2]$, which was used in [17], has these properties.

Since the Gaussian source function approximates a delta function, it is useful for convolution. A given source function may be approximated by

$$F(t) \cong \sum_n a^n G_\nu(t - t^n) \quad (41)$$

provided ν is sufficiently large. The coefficients a^n are determined by requiring the approximation to be exact at the points t^n, which do not necessarily correspond to the grid points t_n and may be spaced irregularly. This constraint gives the following system of equations:

$$F(t^m) = \sum_{n=m-q}^{m+q} a^n G_\nu(t^m - t^n). \quad (42)$$

The matrix corresponding to this system of equations is reduced to the $2q + 1$ diagonals centered about the main diagonal, where q is a small integer, due to the fact that $G_\nu(t)$ decays rapidly away from $t = 0$. In some situations, the approximation given by (41) might be more useful than the Fourier decomposition for approximating broadband source functions because the Gaussian itself is a broadband source function.

VI. PWE Benchmark

The Gaussian source $G_\nu(t)$ with $\nu = 150\ s^{-1}$ is placed at $z_0 = 75$ m in an ocean in which $c = c_0 = 1500$ m/s. Ocean depth is 200 m for $r < 4$ km, linearly decreasing from 200 to 50 m over 4 km $< r <$ 8 km, and 50 m for $r > 8$ km. In the sediment, $c = 1600$ m/s, $\rho = 1.5$ g/cm^3, and $\beta = 0.5$ dB/λ. The grid spacings are $\Delta t = 2.5\ \text{m}/c_0$, $\Delta s = 1$ m, and $\Delta z = 1.5$ m with $s_{\max} = 400$ m and $z_{\max} = 300$ m. An absorbing layer 150 m thick is added below $z = z_{\max}$ over which β increases to prevent reflections. The grid Γ is initialized with the leading Gaussian front at $r = 350$ m and $s = 300$ m.

Fig. 1 contains a sequence of contour plots of the acoustic pressure. The ocean bottom is marked with a solid horizontal line. Solid contours represent $p > 0$; dashed contours represent $p < 0$. The leading front is located about 100 m to the left of the leading end of the grid. The reflection coefficient at the ocean surface is -1. The reflection coefficient at the ocean bottom is approximately -1 for small-angle propagation. Thus, the fronts that trail the leading front and have reflected from the ocean surface and bottom are composed of alternating solid and dashed contours. The signal is essentially confined to Γ, which was assumed in the derivation of the numerical solution.

The leading front is accompanied below the interface by an evanescent wave. This is analogous to the evanescent portions of the normal modes for the time-harmonic problem. The reflected fronts also exhibit this feature. The evanescent tails penetrate deeper into the water for these fronts, which propagate at higher angles. In analogy, the length of the evanescent tails of the normal modes increase with propagation angle. In the upslope region, the evanescent tails grow extremely long and energy penetrates into the sediment. This behavior is analogous to the coupling of energy from the discrete spectrum into the continuous spectrum for the time-harmonic problem as described in [5]. The tails begin to subside in length after the top of the slope is reached.

A time-harmonic source with $\omega = 100\ \pi s^{-1}$ is approximated by

$$\sin(\omega t) \cong 1.267 \sum_n (-1)^n G_\nu \left[\frac{t - \left(n + \frac{1}{2} \right)\pi}{\omega} \right]. \quad (43)$$

The constants $a^n = 1.267 \cdot (-1)^n$ and $t^n = (n + \frac{1}{2})\pi/\omega$ were determined by taking $q = 1$. It is evident from Table I that (43) gives an accurate approximation. By superposition, the time-harmonic response p_{cw} is approximated by

$$p_{cw}(t) \cong 1.267 \sum_n (-1)^n p \left[\frac{t - \left(n + \frac{1}{2} \right)\pi}{\omega} \right] \quad (44)$$

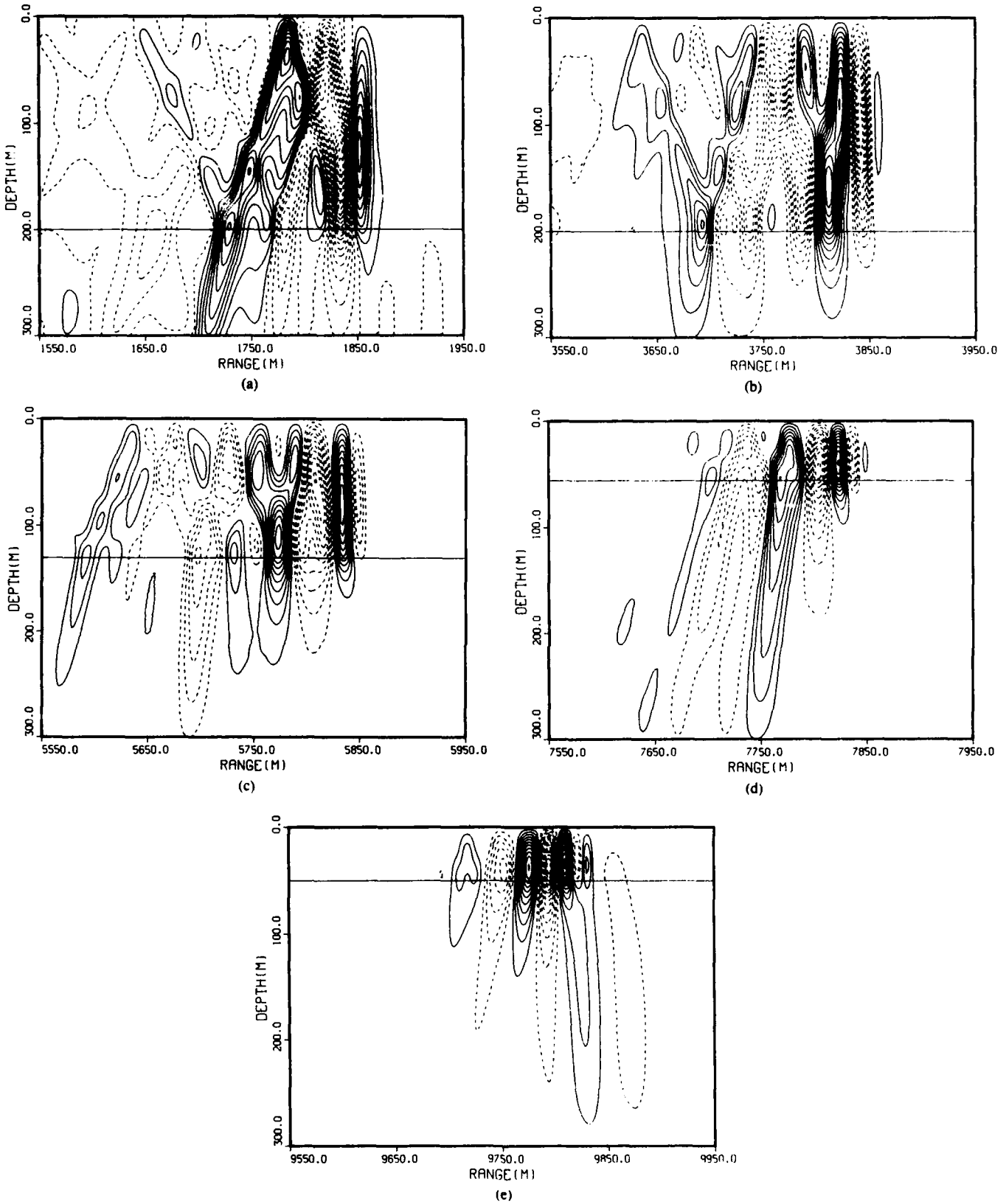

Fig. 1. Sequence of snapshots of the acoustic pressure p for a Gaussian point source. Solid lines represent $p > 0$. Dashed lines represent $p < 0$. Ocean surface is at the top boundary. Solid horizontal line is the ocean bottom. Signal propagates toward the right.

TABLE I
APPROXIMATION OF A SINUSOID BY GAUSSIANS. TWO GAUSSIANS USED PER CYCLE CENTERED AT THE MAXIMA AND MINIMA OF THE SINUSOID

t(ms)	sin (ωt)	$\Sigma a^n G_\nu(t - t^n)$
0.5	0.1564	0.1564
1.0	0.3090	0.3089
1.5	0.4540	0.4539
2.0	0.5878	0.5877
2.5	0.7071	0.7071
3.0	0.8090	0.8091
3.5	0.8910	0.8912
4.0	0.9511	0.9513
4.5	0.9877	0.9880
5.0	1.0000	1.0003

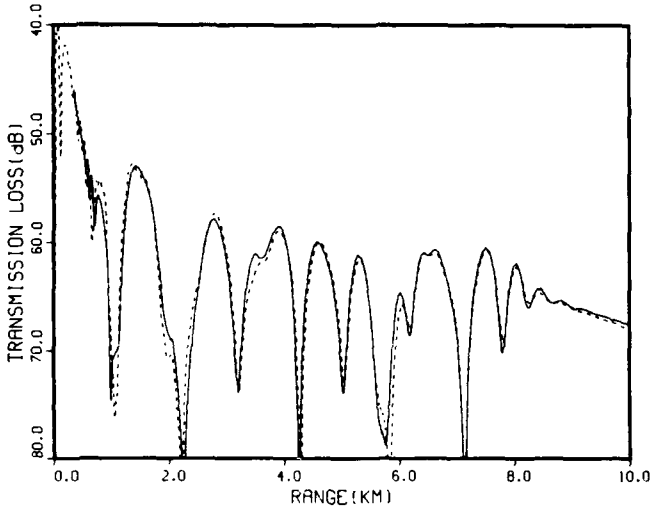

Fig. 2. Benchmark calculation for 50 Hz source. Data for solid curve is generated from a PWE (time-domain) calculation followed by a convolution to approximate the CW response. Data for dashed curve is generated with a PE (frequency-domain) calculation.

where p is the response to the Gaussian. Fig. 2 contains a plot of transmission loss at the receiver depth $z_r = 25$ m calculated using (18) with (44) and using (9). The excellent agreement demonstrates the accuracy of the PWE, the starting field, and the numerical solution.

VII. Conclusions

A model that handles low-frequency, bottom-interacting pulse propagation in the ocean has been derived, and a new initial field has been considered. The PWE accounts for variations in sound speed, density, and attenuation. The attenuation is assumed to depend linearly on frequency in the sediment, although the approach can be generalized to handle an arbitrary dependence. Cylindrical spreading is handled analytically, an additional improvement in the model. A numerical solution for the PWE was derived, and the accuracy of the asymptotics, numerics, and starting field was demonstrated with a benchmark. The numerical solution is based on the approach of [17]. However, the solution has been simplified, and methods designed for linear problems have been implemented. The results presented here should apply to the TDPE.

Further development of the PWE is needed. Future studies to extend the present work might compare the PWE with the TDPE and compare run-times for these models and frequency-domain models. It would be advantageous to extend the model to handle wide-angle propagation, which is known to be important from frequency-domain studies. The causal dispersion law [27] that corresponds to the linear attenuation law should be implemented into the model because dispersion is known to have a significant effect on propagation in solids [23], and the acausal linear attenuation law sometimes gives unsatisfactory predictions for bottom-interacting propagation in the ocean [25].

Acknowledgment

The author thanks G. A. Kriegsmann and E. L. Reiss for their suggestions in supervising this work, which was part of a thesis project at Northwestern University, and the reviewers for their helpful comments and for providing several references.

References

[1] F. D. Tappert, "The parabolic approximation method," in *Wave Propagation and Underwater Acoustics* (Lecture Notes in Physics, Vol. 70), J. B. Keller and J. S. Papadakis, Eds. New York: Springer, 1977, pp. 224-280.

[2] S. T. McDaniel and D. Lee, "A finite-difference treatment of interface conditions for the parabolic equation: The horizontal interface," *J. Acoust. Soc. Amer.*, vol. 71, pp. 855-858, Apr. 1982.

[3] D. Lee and S. T. McDaniel, "A finite-difference treatment of interface conditions for the parabolic equation: The irregular interface," *J. Acoust. Soc. Amer.*, vol. 73, pp. 1441-1447, May 1983.

[4] G. A. Kriegsmann, "A multiscale derivation of a new parabolic equation which includes density variations," *Comp. Maths. Appls.*, vol. 11, nos. 7/8, pp. 817-821, 1985.

[5] F. B. Jensen and W. A. Kuperman, "Sound propagation in a wedge-shaped ocean with a penetrable bottom," *J. Acoust. Soc. Amer.*, vol. 67, pp. 1564-1566, May 1980.

[6] R. N. Baer, "Propagation through a three-dimensional eddy including effects on an array," *J. Acoust. Soc. Amer.*, vol. 69, pp. 70-75, Jan. 1981.

[7] W. L. Seigmann, G. A. Kreigsmann, and D. Lee, "A wide-angle three-dimensional parabolic wave equation," *J. Acoust. Soc. Amer.*, vol. 78, pp. 659-664, Aug. 1985.

[8] D. Lee, Y. Saad, and M. H. Schultz, "An efficient method for solving the three-dimensional wide-angle wave equation," Dept. of Computer Sciences, Yale Univ., New Haven, CT, Research Rep. YALEU/DCS/RR-463, 1986.

[9] J. F. Claerbout, *Fundamentals of Geophysical Data Processing*. New York: McGraw-Hill, 1976, pp. 206-207.

[10] G. Botseas, D. Lee, and K. E. Gilbert, "IFD: Wide-angle capability," NUSC, New London, CT, NUSC Tech. Rep. 6905, 1983.

[11] *NORDA Parabolic Equation Workshop*, J. A. Davis, D. White, and R. C. Cavanagh, Eds., NORDA, NSTL Station, MS, NORDA Tech. Note 143, 1982.

[12] L. Nghiem-Phu and F. D. Tappert, "Modeling of reciprocity in the time domain using the parabolic equation method," *J. Acoust. Soc. Amer.*, vol. 78, pp. 164-171, July 1985.

[13] L. Nghiem-Phu and F. D. Tappert, "Parabolic equation modeling of the effects of ocean currents on sound transmission and reciprocity in the time domain," *J. Acoust. Soc. Amer.*, vol. 78, pp. 642-648, Aug. 1985.

[14] H. Schmidt and G. Tango, "Efficient global matrix approach to the computation of synthetic seismograms," *Geophys. J. Roy. Astron. Soc.*, vol. 84, pp. 331-359, Feb. 1986.

[15] M. G. Brown, "Application of the WKBJ Green's function to acoustic propagation in horizontally stratified oceans," *J. Acoust. Soc. Amer.*, vol. 71, pp. 1427-1432, June 1982.

[16] R. F. Henrick, J. R. Brannan, D. B. Warner, and G. P. Forney, "The uniform WKB modal approach to pulsed and broadband propagation," *J. Acoust. Soc. Amer.*, vol. 74, Nov. 1983.

[17] B. E. McDonald and W. A. Kuperman, "Time domain formulation

for pulse propagation including nonlinear behavior at a caustic," *J. Acoust. Soc. Amer.*, vol. 81, pp. 1406–1417, May 1987.

[18] J. F. Claerbout and A. G. Johnson, "Extrapolation of time dependent waveforms along their path of propagation," *Geophys. J. Roy. Astron. Soc.*, vol. 26, pp. 285–295, Nov. 1971.

[19] J. F. Claerbout, *Fundamentals of Geophysical Data Processing*. New York: McGraw-Hill, 1976, pp. 208–215.

[20] J. E. Murphy, "Finite-difference treatment of a time-domain parabolic equation: Theory," *J. Acoust. Soc. Amer.*, vol. 77, pp. 1958–1960, May 1985.

[21] P. G. Bergmann, "The wave equation in a medium with a variable index of refraction," *J. Acoust. Soc. Amer.*, vol. 17, pp. 329–333, Apr. 1946.

[22] F. J. McDonal *et al.*, "Attenuation of shear and compressional waves in Pierre shale," *Geophysics*, vol. 23, pp. 421–439, July 1958.

[23] P. C. Wuenschel, "Dispersive body waves—An experimental study," *Geophysics*, vol. 15, pp. 539–551, Aug. 1965.

[24] E. L. Hamilton, "Compressional-wave attenuation in marine sediments," *Geophysics*, vol. 37, pp. 620–646, Aug. 1972.

[25] J. Zhou, X. Zhang, P. H. Rogers, and J. Jarzynski, "Geoacoustic parameters in a stratified sea bottom from shallow-water acoustic propagation," *J. Acoust. Soc. Amer.*, vol. 82, pp. 2068–2074, Dec. 1987.

[26] R. D. Stoll, "Marine sediment acoustics," *J. Acoust. Soc. Amer.*, vol. 77, pp. 1789–1799, May 1985.

[27] W. I. Futterman, "Dispersive body waves," *J. Geophys. Res.*, vol. 67, pp. 5279–5291, Dec. 1962.

[28] A. R. Mitchell and D. F. Griffiths, *The Finite Difference Method in Partial Differential Equations*. New York: Wiley, 1980, pp. 164–167.

★

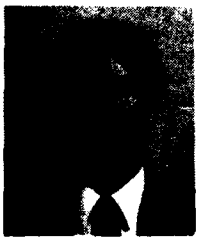

Michael D. Collins was born in Greenville, PA, in 1958. He received the B.S. degree in mathematics from the Massachusetts Institute of Technology, Cambridge, in 1982, the M.S. degree in mathematics from Stanford University, Palo Alto, CA, in 1986, and the Ph.D. degree in applied mathematics from Northwestern University, Evanston, IL, in 1988.

Since 1985 he has worked for the Naval Ocean Research and Development Activity, Stennis Space Center, MS, as both a civilian employee of the Navy and as an on-site representative of SYNTEK Engineering and Computer Systems, Inc., Rockville, MD.

Dr. Collins is a member of the Acoustical Society of America.